Biomedical Signal Processing and Control 83 (2023) 104666

Contents lists available at ScienceDirect

Biomedical Signal Processing and Control

journal homepage: www.elsevier.com/locate/bspc

Directed brain network analysis in anxious and non-anxious depression based on EEG source reconstruction and graph theory

Hesam Shokouh Alaei [a,b], Majid Ghoshuni [a,*], Iraj Vosough [a]

[a] Department of Biomedical Engineering, Mashhad Branch, Islamic Azad University, Mashhad, Iran
[b] Centre for Biomedical Engineering, School of Mechanical Engineering Sciences, University of Surrey, Guildford, United Kingdom

ARTICLE INFO

Keywords:
Directed brain network
Graph theory
EEG source localization
Major depressive disorder (MDD)
Effective connectivity

ABSTRACT

Patients with anxious depression have more severe symptoms, more side effects, and higher resistance to treatment than patients with non-anxious depression; therefore, it is crucial to clarify the differences between these two types of patients. In this study, a 5-minute resting EEG was recorded in 15 patients with anxious depression and 9 patients with non-anxious depression under eyes open and closed conditions. Sixty-eight subcortical regions were extracted using exact low resolution brain electromagnetic tomography (eLORETA). The directed transfer function was then used to construct brain networks. Specific features based on graph theory including the strength of connectivity and betweenness centrality (BC) were calculated from the networks. Finally, significant features were selected using the Mann-Whitney *U* test, and patients were classified into anxious and non-anxious depressive groups using the Support Vector Machine (SVM). Results showed that features of outward connectivity strength led to the highest accuracy, F-score, and specificity with 91.66%, 87.5%, and 100% in the eyes-closed state, respectively. Moreover, we found that the strength of connectivity in both directions increased for the anxious depressive group during the eyes-open state. In particular, higher outward connectivity was observed in the right hemisphere for the anxious depressive group. Further findings also revealed that features with the most significant difference were mainly associated with the beta band. In addition, significant increased inward and outward connectivity and decreased nodal centrality were observed in the posterior regions of the default mode network. These preliminary findings might provide new insights into the recognition of anxious depressed patients.

1. Introduction

Major depressive disorder (MDD) affects 6% of the global adult population annually and is one of the most prevalent psychiatric disorders [1]. About half of MDD patients also have anxiety, such as social anxiety disorder (SAD), generalized anxiety disorder (GAD), or panic disorder (PD) [2]. When MDD co-occurs with anxiety, the risk of suicide becomes greater, and patients may require long-term treatment [3,4]. Currently, however, there is a lack of accepted treatment for patients with anxious depression. They usually receive the same treatment strategies that are given for depression or anxiety. Consequently, the rate of treatment resistance is higher for them than for patients with pure depression or anxiety [5]. Moreover, the rate of medical utilization increased rapidly for patients with comorbid depression and anxiety [4]. Therefore, it is necessary to distinguish anxious depressed patients from non-anxious depressed patients in order to improve diagnosis and treatment methods.

Some studies have examined the underlying biology of MDD using neuroimaging techniques. However, the majority of these works failed to consider the comorbidity of anxiety. Accordingly, we reviewed studies that considered the effects of co-occurring anxiety on depression. van Tol et al. [6], showed a general hyporesponse at the right hippocampus during a word-recognition task. Also, they demonstrated a general reduced rostral-dorsal anterior cingulate volume in MDD patients with or without anxiety [7]. They also found a higher left dorsolateral prefrontal activity during a visual task in the MDD group compared to the healthy control group [8]. In another study, a lower blood oxygen-level-dependent signal was observed at the middle frontal gyrus in the MDD group, whereas no relation was found between depression and anxiety symptoms [9]. A small number of studies have successfully found significant differences in patients with anxious and non-anxious depression based on an fMRI dataset. The main findings

* Corresponding author.
E-mail address: ghoshuni@mshdiau.ac.ir (M. Ghoshuni).

https://doi.org/10.1016/j.bspc.2023.104666
Received 15 August 2021; Received in revised form 12 January 2023; Accepted 31 January 2023
Available online 7 February 2023

consisted of higher activity of the insula, and dorsolateral prefrontal as well as a reduced volume of right medial orbitofrontal, right fusiform, left temporal pole and left lateral occipital cortices in patients with anxious depression [10,11]. Another study showed increased thickness of the left cingulate, right medial frontal gyri, and left paracentral lobe in anxious depressed patients compared to non-anxious depressed patients [12].

A few fMRI studies examined the abnormalities of neural circuits in anxious depressions using connectivity analysis. In a particular study, the default-mode network (DMN) was investigated in elderly patients with anxious depression [13]. Their reports exhibited increased functional connectivity in the posterior regions of DMN, and a decreased connectivity in the anterior regions of DMN in depressed elderly patients with high anxiety [13]. As for the limbic network, the functional connectivity in the anxious depressive group increased significantly [14]. Concerning the amygdala network, bilateral functional connectivity significantly decreased in patients with anxious depression [15], whereas bilateral structural connectivity did not differ [16].

Other neuroimaging studies have been carried out based on electroencephalography (EEG). Most of them showed evidence of greater neural activity in the right frontal region in depressed patients with anxiety [17–19]. Nevertheless, some findings showed a lower alpha power in the right posterior regions [20], higher activity in the right parieto-temporal lobe [21], a higher high-beta power in the posterior regions for the anxious depressive group [22], and higher beta power in the fronto-temporal lobe for the non-anxious depressive group [23]. Even so, there is an EEG study that did not find any significant differences between anxious depressive groups and healthy controls [24]. Other EEG studies have investigated the subcortical regions by quantitative EEG (QEEG) and Low Resolution Electromagnetic Tomography (LORETA). By using such techniques, the cingulate, precuneus, and some regions of the frontal lobe (e.g., right superior and inferior frontal gyri, and orbitofrontal cortex) were found to have abnormalities in MDD patients with or without anxiety [18,25].

Evidence from the EEG studies indicates that there is a lack of brain connectivity analysis regarding anxious depressive disorder. On the contrary, disruption in the brain network of MDD patients with anxiety was mainly assessed by the fMRI studies based on functional or structural connectivity. Nonetheless, these analyses only consider the undirected brain network, and directed interactions between cortical regions are disregarded [26]. Effective connectivity, on the other hand, can provide information about the direction of information flow in the brain network [27]. In this study, the causal interactions using the effective connectivity analysis based on the resting EEG recorded from anxious and non-anxious depressed patients in eyes open and closed conditions have been investigated. The constructed brain network was then analyzed by graph theory metric to estimate the strength and the centrality of each node. The graph features were also estimated for EEG frequency bands since the effect of MDD with comorbid anxiety on various frequency bands has been poorly understood, although some research suggests that alpha and theta bands could be possible biomarkers that distinguish MDD from anxiety [28,29]. Several studies have been carried out to explore brain connectivity based on scalp EEG electrodes. However, many scalp sensors might collect the activity originating from the same brain sources, as a result of which multivariate analysis between pairs of EEG channels may produce an inaccurate brain network [30]. Due to this reason, we reconstructed the brain sources on the multiple subcortical regions from the surface EEG using a source reconstruction method called “exact low resolution brain electromagnetic tomography” (eLORETA) before brain connectivity estimation. eLORETA is a genuine inverse solution that provides exact zero localization error in the presence of biological and measurement noise [31]. Following EEG source connectivity estimation, the regions and frequency bands that showed statistically significant differences in terms of connectivity strength and centrality were identified by statistical analysis. The observed regions were also examined in the DMN to study how the connectivity changes are reflected in an active large-scale brain network during the resting state. Finally, a classification was employed to distinguish between patients with anxious and non-anxious depression.

The next section of this paper, Section 2, is devoted to describing the details of EEG recording and signal processing stage including source reconstruction, estimation of effective connectivity, graph theory analysis, feature extraction, and classification. The findings of the proposed method are presented in Section 3, and the discussion and conclusion are explained in Sections 4 and 5, respectively.

2. Materials and methods

2.1. Participants and psychiatric assessment

Twenty-four patients (20 females and 4 males, mean age: 30.08 ± 14.38) with MDD participated in this study. All patients were assessed with the Symptom CheckList-90 (SCL90). SCL90 is a 90-item questionnaire that roughly takes 12–15 min and is scored on a scale from 0 to 4 [32]. Despite the depression, anxiety was also considered to determine whether it is comorbid with the depression or not. A summary of patient characteristics and their scores related to depression and anxiety is given in Table 1. According to the scores, 15 patients were grouped as anxious depression, and 9 patients were grouped as non-anxious depression.

2.2. EEG recording and preprocessing

EEG data were recorded by Mitsar-EEG 201 system with a sampling rate of 250 Hz and 19 channels (FP1, FP2, F3, F4, C3, C4, P3, P4, O1, O2, F7, F8, T3, T4, T5, T6, Fz, Cz, Pz) according to the international 10–20 electrode system with the linked-ears reference. The data of each patient was collected for 5 min in a resting state under eyes open and closed conditions. The NeuroGuide software v.3.1 was then used to filter the noises and unwanted frequencies using a 0.5–40 Hz band-pass filter. This software was also used to remove physiological and non-physiological artifacts semi-automatically. In this manner, some arbitrarily artifact-free EEG samples were selected manually, afterwards, NeuroGuide automatically rejected the artifacts from the whole EEG signal based on the selected segments.

2.3. EEG analysis overview

The pipeline of the proposed methodology is depicted in Fig. 1. It is mainly divided into three parts. In the first part, 19-channel filtered EEG signals on the scalp level are transformed into new signals on the cerebral cortex level using the EEG source reconstruction technique including forward modeling and inverse modeling. In the second part, the causal interactions (effective connectivity) between all reconstructed signals are computed. In addition, the brain network analysis is applied to obtain a set of features for each patient. In the last part, a classifier is utilized to distinguish the anxious and non-anxious depressive groups based on the selected features obtained from graph analysis. The details of each part are explained in the following sections.

Table 1
Patient characteristics, and results of the SCL90 test for depression and anxiety disorders.

Group	No. of patients	Mean age	Mean SCL90 Score	
			Depression	Anxiety
Anxious Depression	15 (F:12, M:3)	22.66 ± 7.48	3.21 ± 0.37	3.14 ± 0.35
Non-Anxious Depression	9 (F: 8, M: 1)	42.44 ± 14.89	3.04 ± 0.24	1.76 ± 0.45

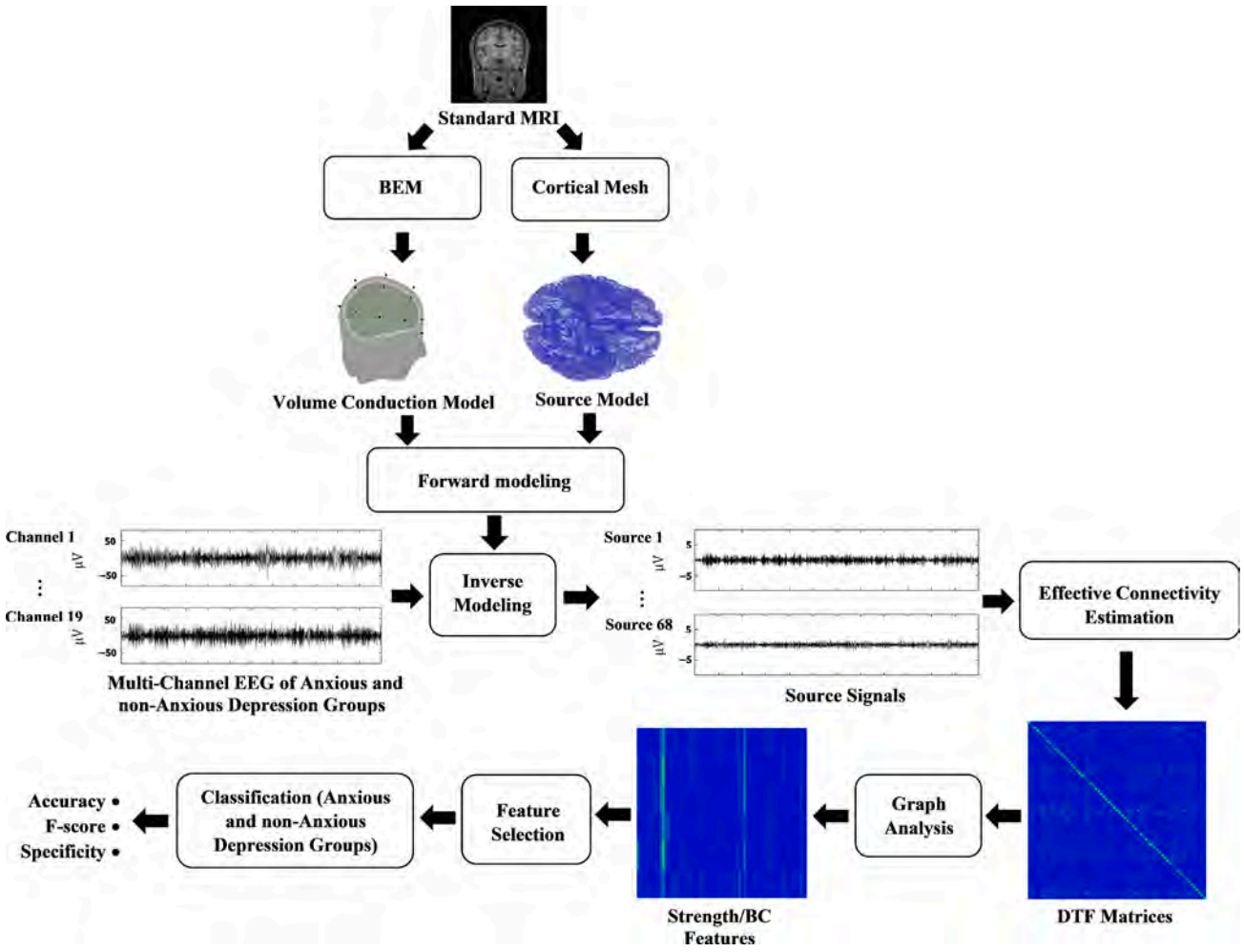

Fig. 1. Block diagram of the proposed method. (BEM: boundary element method, DTF: directed transfer function, BC: betweenness centrality).

2.4. EEG source reconstruction

Generally, all EEG source reconstruction methods consist of forward and inverse modeling [33]. The forward modeling defines how electrophysiological sources project to the electrical potentials on the scalp through volume conduction, whereas the inverse modeling finds a solution for the sources given scalp potentials and volume conduction [33]. As we expected, the amplitude of the filtered EEG signal decreased remarkably after the inverse modeling due to the linear combination of source activities (see Fig. 1).

2.4.1. Forward modeling

For forward modeling, it is essential to estimate potential or field distribution on the scalp known as the Lead Field matrix. Volume conductor, source model, and electrode positions are required to compute the lead field matrix. These three elements represent the geometrical and electrical properties of the head that were derived from a standard high-resolution MRI downloaded from the FieldTrip FTP server (ftp://ftp.fieldtriptoolbox.org/pub/fieldtrip/tutorial/Subject01.zip). To create a volume conduction model, firstly, the anatomical MRI was segmented into the scalp, skull, and brain tissue. Each surface is then modeled via vertices and triangles. Finally, the boundary element method (BEM), as a numerical computational method, was used to create the head model [34]. Electrode positions were subsequently aligned on the surface of the head model. It is worth mentioning that the creation of the head model using BEM was done by the FieldTrip toolbox in MATLAB R2020a [35].

To create a source model based on the template MRI, FreeSurfer v.7.1.1 was used [36]. This software converts the 3D MRI to the 2D triangulated cortical mesh using a series of steps including skull stripping, volume segmentation, estimation of white matter boundary, gray matter thickness, extraction of cortical mesh, and processing of surface mesh. These steps mostly run automatically, however, in this study, the brain stem was not fully removed by FreeSurfer, thus an intervention was required to remove it manually. FreeSurfer usually creates meshes with over 100,000 vertices per hemisphere which is too much for the EEG source reconstruction. As a result, the Connectome Workbench software v.1.5 was employed to reduce the number of vertices to 8000 vertices (4000 per hemisphere). Finally, the lead field matrix is calculated for each vertex (voxel) taking into account the head model and the channel positions. The whole process of forward modeling was implemented only once for all patients.

2.4.2. Inverse modeling

In current study, eLORETA was adopted as a promising source localization method. Consider the inverse model as:

$$\widehat{j}_i = T_i Y \tag{1}$$

where $Y \in \mathbb{R}^{N_E \times N_n}$ denotes the EEG measured by N_E scalp electrodes and N_n time samples. $\widehat{j}_i \in \mathbb{R}^{3 \times N_n}$ is the virtual channel of x-, y- and z-component of the equivalent current dipole at the i th voxel ($i = 1, \cdots, N_V$). Moreover, $T_i \in \mathbb{R}^{3 \times N_E}$ is a transformation matrix (spatial filter) related to the i th voxel that is computed by a weighted minimum norm

solution:

$$T_i = w_i^{-1} L_i^T \left(LW^{-1}L^T + \alpha H\right)^+ \tag{2}$$

where L is the lead field matrix estimated from forward modeling, $W \in \mathbb{R}^{(3N_V)\times(3N_V)}$ is the symmetric weight matrix that has non-zero diagonal entities as $w_i \in \mathbb{R}^{3\times 3}$ for each voxel, $\alpha \geq 0$ is the regularization parameter, and H, known as centering matrix, is an average reference operator defined as:

$$H = \mathrm{I} - \frac{11^T}{1^T 1} \tag{3}$$

Here, $\mathrm{I} \in \mathbb{R}^{N_E \times N_E}$ is the identity matrix, and $1 \in \mathbb{R}^{N_E \times 1}$ is a vector of ones. Note that superscript '$+$' in Eq. (2) denotes the Moore-Penrose pseudoinverse which is equal to the common inverse if the $(\bullet)$ is non-singular.

Assume that W is initialized as an identity matrix (i.e., $w_i = 1$ for $i = 1, \cdots, N_V$), then the weights of eLORETA are updated in an iterative equation as follows until the change in the weight matrix becomes negligible:

$$w_i = \left[L_i^T \left(LW^{-1}L^T + \alpha H\right)^+ L_i\right]^{1/2} \tag{4}$$

Finally, the updated W is plugged into the Eq. (2) to compute the transformation matrix, so that the new time-series in three dimensions for every dipole (i.e., 8000 dipoles) are obtained by Eq. (1).

2.4.3. Dimension reduction

Connectivity analysis between triplets of 8000 virtual channels makes the interpretation of results substantially difficult. To tackle this problem, the created triple signals at each dipole were firstly projected along an orientation that explains most variance using the singular value decomposition to find the largest eigenvector. Then, the number of new one-dimensional signals decreased to 68 signals representing the neural activity of 68 regions of interest (ROI) obtained from the Desikan-Killiany atlas [37]. It should be pointed out that the time course of each region was simply estimated by averaging time-series within their region.

2.5. Brain connectivity analysis

This important section is referred to as feature extraction in which the neural activities of subcortical regions are turned into a set of features characterizing the pair-wise connections between ROIs. Such features can be represented in a square matrix whose rows and columns indicate network nodes, and entries indicate network links (edges) [30]. In this study, the number of nodes is equal to 68, and links were estimated using an effective connectivity method. Once the nodes and edges were obtained, we analyzed the network properties via the brain connectivity toolbox (BCT) [38].

2.5.1. Weighted directed network

Effective connectivity is known for the description of directional influence or causal interaction between pair-wise signals. Unlike functional connectivity, this method yields a non-symmetric matrix, meaning that the information flow from signal i to signal j is different than from signal j to signal i [39]. Several effective connectivity measures have been proposed based on the multivariate autoregressive model (MVAR). The directed transfer function (DTF) is one of the MVAR-based measures that was utilized in this study [40].

Once the time-series, $X \in \mathbb{R}^{N_{ROI}\times N_n}$, are reconstructed ($N_{ROI} = 68$), the MVAR with order p for $n = p+1, \cdots, N_n$ can be defined as:

$$\sum_{r=0}^{p} A(r)X(n-r) = E(n) \tag{5}$$

where $A(r) \in \mathbb{R}^{N_{ROI}\times N_{ROI}}$ with $A(0) = \mathrm{I}$ denotes model coefficients, and $E \in \mathbb{R}^{N_{ROI}\times N_n}$ is multivariate zero mean uncorrelated white noise. The unknown parameters of Eq. (5) were calculated using the ARFIT toolbox. Specifically, $A(1), \cdots, A(p)$ and E are estimated through the Stepwise Least Squares algorithm, and p is approximated based on Schwarz's Bayesian criterion [41].

If the MVAR is transformed into the frequency domain, Eq. (5) can be rewritten in the following form:

$$X(f) = H(f)E(f) \tag{6}$$

where $H(f)$ denotes transfer function which is given by:

$$H(f) = \left(\sum_{r=0}^{p} A(r)e^{-j2\pi f \Delta n}\right)^{-1} \tag{7}$$

Assume that the elements of transfer function are $H_{ij}(f)$ indicating the casual influence from node j to node i at frequency f, then DTF is equal to $\left|H_{ij}(f)\right|^2$. However, DTF is usually determined by its normalized version:

$$\gamma_{ij}^2(f) = \frac{\left|H_{ij}(f)\right|^2}{\sum_{m=1}^{N_{ROI}} |H_{im}(f)|^2} \tag{8}$$

As a result, the $\gamma_{ij}^2(f)$ ranges from 0 to 1 yielding a ratio of in-flow from j th node to i th node with respect to all in-flows to node i at f frequency.

Some recent studies have shown that the connectivity links are proportional to the inverse of the square distance between nodes [42]. Whereas most connectivity measures such as DTF did not take into account the geometric distance in brain networks. According to Eq. (9), we address this problem by producing a weight matrix, $\widehat{w}$, the elements of which are Euclidean distance between node i and node j so that the inverse of this matrix is multiplied with the directed matrix, $\gamma^2(f)$, to obtain a weighted directed matrix, $\widehat{\gamma}^2(f) \in \mathbb{R}^{N_{ROI}\times N_{ROI}}$.

$$\widehat{\gamma}^2(f) = \widehat{w}^{-1}\gamma^2(f) \tag{9}$$

where $\odot$ denotes element-wise product. Concerning the frequency bands of EEG, delta (0.5–4 Hz), theta (4–8 Hz), alpha (8–12 Hz), beta 1 (12–15 Hz), beta 2 (15–18 Hz), and beta 3 (18–25 Hz), the $\widehat{\gamma}^2(f)$ was calculated only for the median of each band instead of computing for all frequencies.

2.5.2. Network metrics

Network analyses provide structural and functional information about the network. BCT is a well-known toolbox that utilizes graph theory to measure the graph in terms of global and local properties [38]. Global measures produce a single value per network, whereas local measures assign a value for each node. In other words, a vector with the length of the number of nodes per network is generated.

Before network evaluation, the weighted directed network matrix should be normalized while should not contain self-connectivity, namely, the weight of nodes on the main diagonal should be 0. After that, we used two local metrics: node strength and betweenness centrality (BC). Node strength is the sum of the entire links connected to a node. As in this case, we deal with the weighted directed matrix, thus, inward links (sum of all columns) and outward links (sum of all rows) are computed separately. On the other hand, the BC is used to identify the important nodes that play a critical role in the coordination of information flow and serve as the bridge from one node to the others. The BC of node i can be computed as:

$$b_i = \frac{1}{(N_{ROI}-1)(N_{ROI}-2)} \sum_{h\neq j, h\neq i, j\neq i} \frac{\rho_{hj}(i)}{\rho_{hj}} \tag{10}$$

where ρ_{hj} denotes total number of shortest paths between node h and node j, and $\rho_{hj}(i)$ is the number of shortest paths between node h and

node *j* that pass through the node *i*.

2.6. Feature selection

So far, three feature vectors derived from in-strength, out-strength, and BC with a length of N_{ROI} have been calculated in six frequency bands. In other words, the size of the feature matrix per network metric is $15 \times 6 \times 68$ (patients $\times$ frequency bands $\times$ regions) for the anxious depressive group and $9 \times 6 \times 68$ (patients $\times$ frequency bands $\times$ regions) for the non-anxious depressive group. In the next stage, we employed the Mann-Whitney *U* test to compare the statistical differences between two feature matrices. The features showing a significant difference ($p < 0.05$) are then selected as discriminant features. Consequently, the size of the feature matrix for each network metric and state of recording was

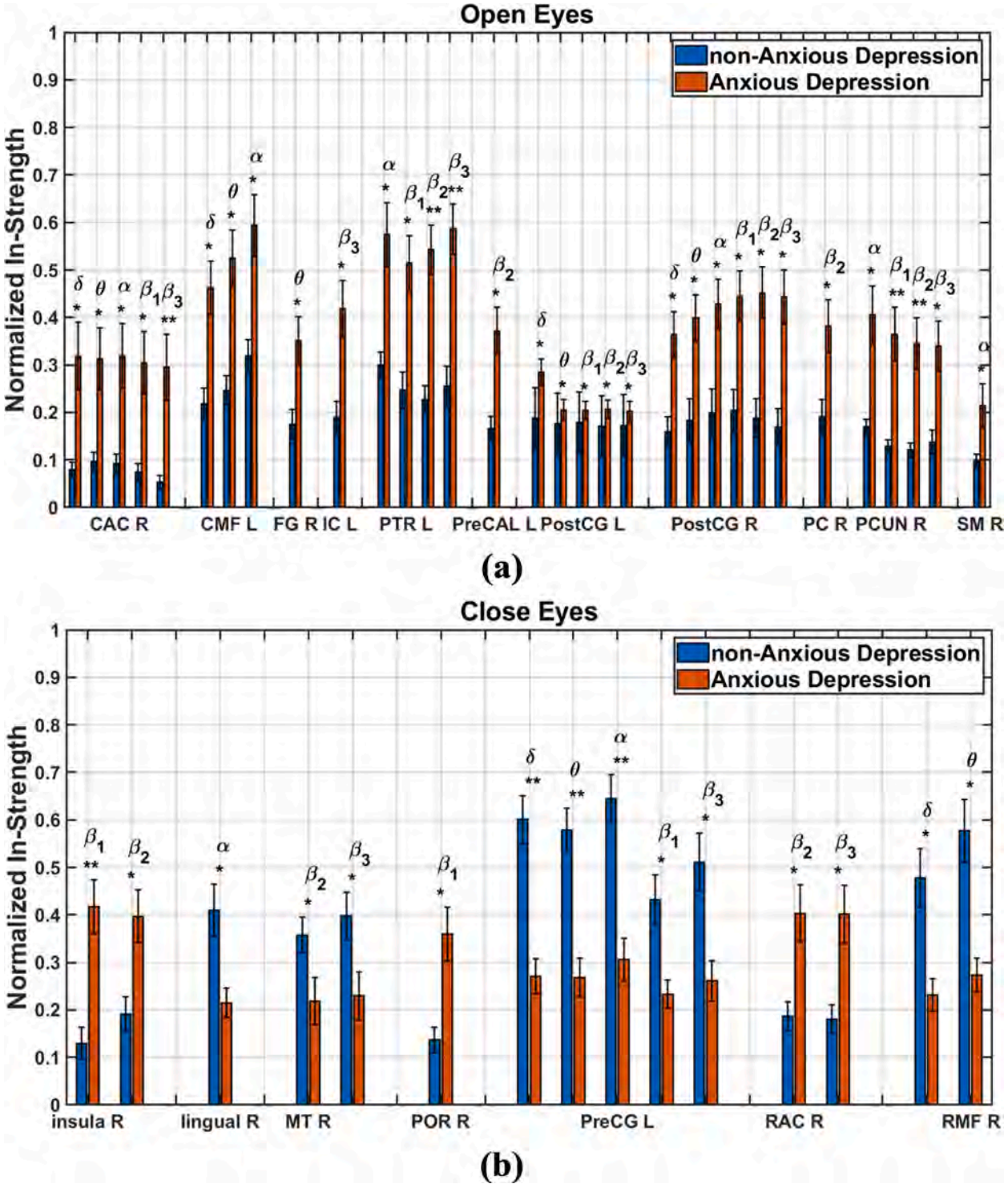

Fig. 2. Bar plot of selected in-strength features for eyes-open condition (a) and eyes-closed condition (b). Single asterisk denotes $p < 0.05$, and double asterisks denote $p < 0.01$. (CAC: caudal anterior cingulate cortex, CMF: caudal middle frontal gyrus, FG: fusiform gyrus, IC: isthmus cingulate gyrus, PTR: pars triangularis, PreCAL: pericalcarine, PostCG: postcentral gyrus, PC: posterior cingulate cortex, PCUN: precuneus, SM: supramarginal gyrus, MT: middle temporal gyrus, POR: pars orbitalis, PreCG: precentral gyrus, RAC: rostral anterior cingulate cortex, RMF: rostral middle frontal gyrus).

reduced to a 2D matrix (patients × optimal features) which was used as an input to the classifier.

2.7. Classification

The selected features must be evaluated to explore to what extent they separate the anxious depressive group from the non-anxious depressive group. To this end, the support vector machine (SVM) with the linear kernel was applied to selected features for each network feature and state of recording. Following model training, the SVM was tested based on the leave-one-out cross-validation (LOOCV) to measure its performance using accuracy (Acc), F-score (F1), and specificity (Spe) which are defined as follows:

$$Acc = \frac{TP + TN}{TP + FN + TN + FP} \times 100\% \tag{11}$$

$$F1 = \frac{2TP}{2TP + FP + FN} \times 100\% \tag{12}$$

$$Spe = \frac{TN}{TN + FP} \times 100\% \tag{13}$$

where *TP*, *TN*, *FP*, and *FN* denote true positive, true negative, false positive and false negative, respectively.

To avoid information leakage between testing and training sets, the feature selection was performed only on the training sets in each fold of LOOCV while discriminant features of testing sets were chosen based on the corresponding selected features of training sets.

3. Results

3.1. Strengths of connectivity

3.1.1. In-Strength features

Concerning node strength of inward links, the features showing significant differences between anxious and non-anxious depressive groups are depicted in Fig. 2 for open and closed eyes conditions. All features were normalized between 0 and 1 to compare the groups more accurately. According to Fig. 2(a), all in-strength values for the anxious depressive group in the eyes-open condition are higher than for the non-anxious depressive group. Among them, the right postcentral gyrus (PostCG) in all frequency bands and the left PostCG in all bands except for the alpha band differ at the significance level of 0.05 with $U_R = 227.1$ and $U_L = 225.6$ using the Mann-Whitney U statistics. Moreover, the features that showed significant difference with $p < 0.01$ can be observed in beta bands (beta 1, beta 2, and beta 3) at the right caudal anterior cingulate cortex (CAC) ($U = 235$), the right precuneus (PCUN) ($U = 223$) and the left pars triangularis (PTR) ($U = 229.5$). In contrast, as can be seen in Fig. 2(b), fewer features were selected for the eyes-closed condition. The left precentral gyrus (PreCG) showed significance with $p < 0.01$ in delta, theta and alpha bands ($U = 141.1$) and with $p < 0.05$ in beta 1 and beta 3 bands ($U = 153$). Other features demonstrated statistical significance across the right hemisphere ($U = 178.3$, $p < 0.05$) including the right insula in beta 1 ($U = 221$, $p < 0.01$).

To investigate the in-strength changes between anxious and non-anxious depressive groups for all ROIs, the brain maps of percent changes are illustrated in Fig. 3. Herein, the average in-strengths across all frequency bands were computed, then the high contrast ROIs were identified using the Mann-Whitney U test. A significant increase is shown by the red contour, while a significant reduction is illustrated by blue contour ($p < 0.05$). For eyes-open recording (Fig. 3(a)), the average in-strengths of six regions related to the anxious depressive group were significantly higher than the non-anxious depressive group: bilateral PostCG ($U_R = 231$ $U_L = 221$), right CAC ($U = 235$), left caudal middle frontal gyrus (CMF) ($U = 213$), left PTR ($U = 234$) and right PCUN ($U = 223$). For eyes-closed recording, the left PreCG ($U = 153$) was the only region that showed a significant decrease in Fig. 3(b). It is worth mentioning that some ROIs such as the cingulate cortex cannot be seen in Fig. 3, as they can be observed in medial views of the brain.

3.1.2. Out-strength features

Similar to the interpretation of in-strength analysis, the bar plot of the significant out-strength features for both conditions is shown in Fig. 4. However, due to the high number of significant features ($p < 0.05$) for the eyes-open state, only features with $p < 0.01$ were

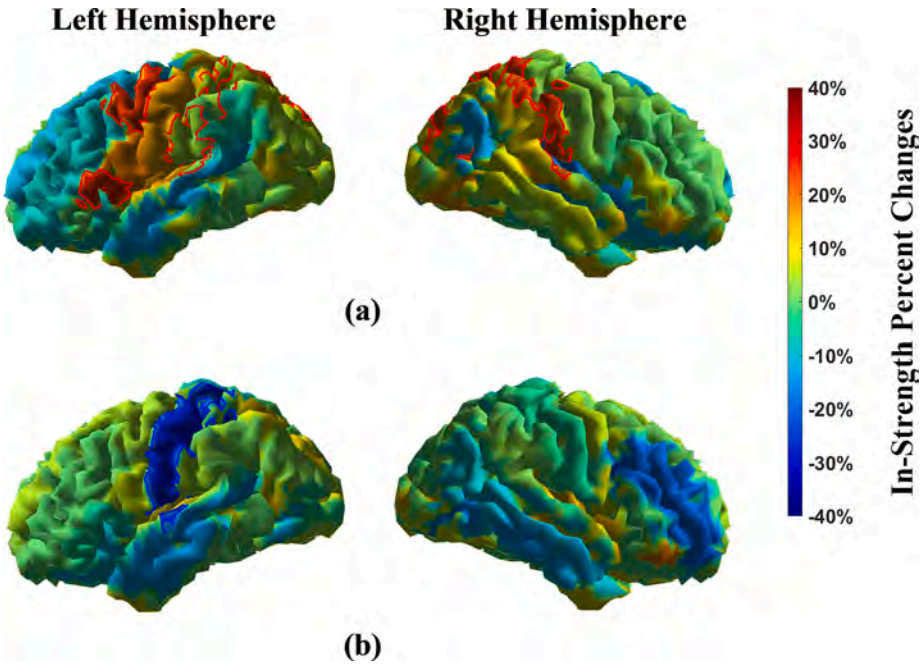

Fig. 3. Brain map of in-strength percentage changes between anxious and non-anxious depressive groups for eyes-open condition (a) and eyes-closed condition (b). The regions showing significant differences are enclosed with red and blue contours ($p < 0.05$). (For interpretation of the references to colour in this figure legend, the reader is referred to the web version of this article.)

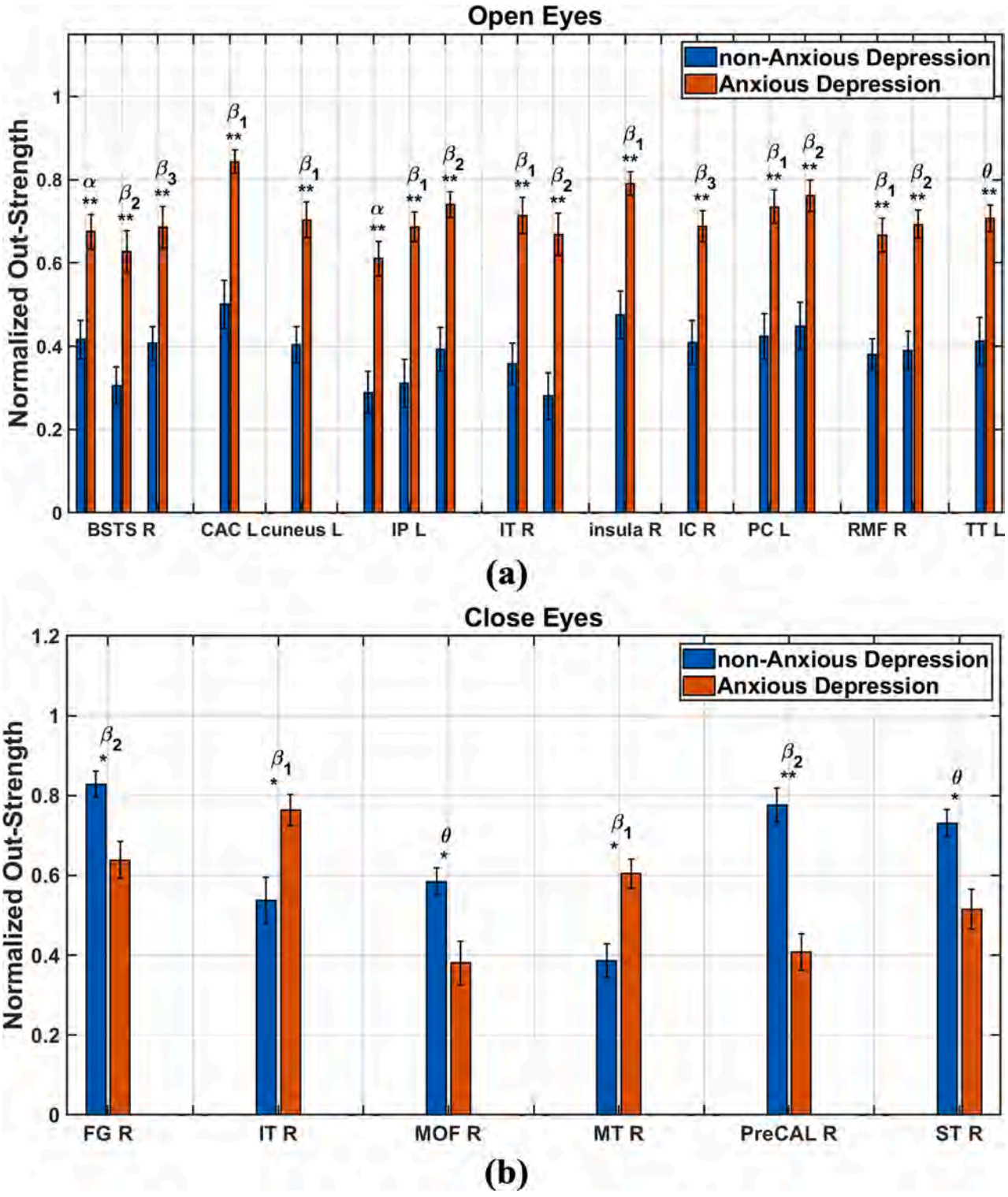

Fig. 4. Bar plot of selected out-strength features for eyes-open condition (a) and eyes-closed condition (b). Single asterisk denotes $p < 0.05$, and double asterisks denote $p < 0.01$. (BSTS: banks of superior temporal sulcus, CAC: caudal anterior cingulate cortex, IP: inferior parietal gyrus, IT: inferior temporal gyrus, IC: isthmus cingulate gyrus, PC: posterior cingulate cortex, RMF: rostral middle frontal gyrus, TT: transverse temporal gyrus, FG: fusiform gyrus, MOF: medial orbitofrontal cortex, MT: middle temporal gyrus, PreCAL: pericalcarine, ST: superior temporal gyrus).

considered for further analysis. It can be seen in Fig. 4(a) that 10 ROIs for the anxious depressive group are higher than for the non-anxious depressive group during eyes-open recording, and they consist of the banks of the superior temporal sulcus (BSTS) ($U = 223.6$), the inferior temporal gyrus (IT) ($U = 235.5$), the insula ($U = 233$), the isthmus cingulate gyrus (IC) ($U = 232$) and the rostral middle frontal gyrus (RMF) ($U = 235.5$) in the right hemisphere as well as the CAC ($U = 238$), the cuneus ($U = 235$), the inferior parietal gyrus (IP) ($U = 234$), the posterior cingulate cortex (PC) ($U = 235.5$) and the transverse temporal gyrus (TT) ($U = 232$) in the left hemisphere. Interestingly, 14 out of 17 features showed significant differences in beta bands ($p < 0.01$). During the close eyes-condition (Fig. 4(b)), six features were selected in the

right hemisphere in which the pericalcarine (PreCAL) was the only region that was significantly different with $p < 0.01$ ($U = 137$) in the beta 2, whereas the fusiform (FG) ($U = 153$), the IT ($U = 222$), the medial orbitofrontal cortex (MOF) ($U = 149$), the middle temporal gyrus (MT) ($U = 230$) and the superior temporal gyrus (ST) ($U = 150$) did differ at the $p < 0.05$ level in the beta 2, beta 1, theta, beta 1 and theta bands, respectively.

Similarly, it is clear from Fig. 5(a) that the out-strength values for the anxious depressive group over almost every cortical region, especially within the right hemisphere, are higher than for the non-anxious depressive group during eyes-open recording. Generally, in the right hemisphere, 45.73% of temporal lobe ($U = 229$), 43.40% of frontal lobe ($U = 215.8$), 48.62% of parietal-occipital lobe ($U = 219$), 23.63% of cingulate cortex ($U = 232$) and insula cortex ($U = 222$) showed significant higher out-strength in the anxious depressive group compared to the non-anxious depressive group ($p < 0.05$), whereas in the left hemisphere, 4.52% of temporal lobe ($U = 221$), 5.17% of frontal lobe ($U = 221$), 27.63% of parietal-occipital lobe ($U = 214.3$) and 52.80% of cingulate cortex ($U = 222$) accounted for the significant out-strength increase in the anxious depressive group. Conversely, Fig. 5(b) reveals that there were no significant changes during the eyes-closed state. However, some areas showed small changes of roughly ± 10% in the right hemisphere.

3.2. Betweenness centrality features

To find out which nodes were altered in terms of centrality, the same approach as the node strengths was adopted. Fig. 6 indicates that both conditions had the same number of significant BC features. For the eyes-open condition (Fig. 6(a)), 15 features were selected in the beta bands against 2 features (left lateral occipital sulcus (LO) and lateral orbitofrontal cortex (LOF)) in the delta band with $p < 0.05$. Left RMF was the only region that showed significant contrast in beta 1, beta 2, and beta 3. Furthermore, five ROIs in the left hemisphere for the anxious depressive group (superior frontal gyrus (SF), RMF, PreCG, LO, and IT) had higher BC than for the non-anxious depressive group. In contrast, four regions in the right hemisphere for the non-anxious depressive group (BSTS, lingual gyrus, pars orbitalis (POR), supramarginal gyrus (SM)) showed significantly higher BC except for the LOF, and the parahippocampal gyrus (PH). As for the eyes-closed condition (Fig. 6(b)), 12 ROIs mainly in delta and beta bands showed significantly higher BC in the non-anxious depressive group. Furthermore, the left superior parietal (SP) ($U = 141$) and the bilateral rostral anterior cingulate cortex (RAC) ($U_R = 140$ $U_L = 137$) in delta band along with the left IC ($U = 139$) and the right lingual gyrus ($U = 228$) in beta 2 band showed significant difference with $p < 0.01$.

The average BC differences between anxious and non-anxious depressive groups are shown in Fig. 7. Due to inconsistent BC contrast in the frequency bands, fewer mean significant changes can be seen across the anatomical regions. During the eyes-open recording (Fig. 7 (a)), the left SP ($U = 217$) represents considerable higher BC for the anxious depressive group, whereas significant lower BC was observed at the left PostCG ($U = 158.5$). On the other hand, according to Fig. 7(b), a significant BC increase was observed in the right lingual gyrus ($U = 188.5$), and considerable reduced BC was observed on the right insula cortex ($U = 158.5$) during the eyes-closed condition.

3.3. Default mode network analysis

Irrespective of the frequency bands or the state of data recording, the spatial anatomy of brain regions with significant network changes ($p < 0.05$) are depicted across the regions of DMN in Fig. 8 for in-strength, out-strength, and BC features separately. This figure reveals that various nodes (regions) of DMN such as medial prefrontal (medial orbitofrontal cortex and rostral anterior cingulate), medial and lateral parietal (posterior cingulate, precuneus, inferior parietal, supramarginal, and isthmus cingulate gyri), temporal cortices (the middle temporal gyrus), and parahippocampal gyrus are affected by changes in connectivity strength and BC between two groups of patient. As illustrated in Fig. 8(a, b), higher significant strength connectivity, mostly out-strength, can be observed in the medial and lateral parietal for anxious depressive individuals. This increased connectivity is frequently seen in the right hemisphere comprising more nodes of the posterior regions of DMN. However, connectivity strength in a few nodes, namely,

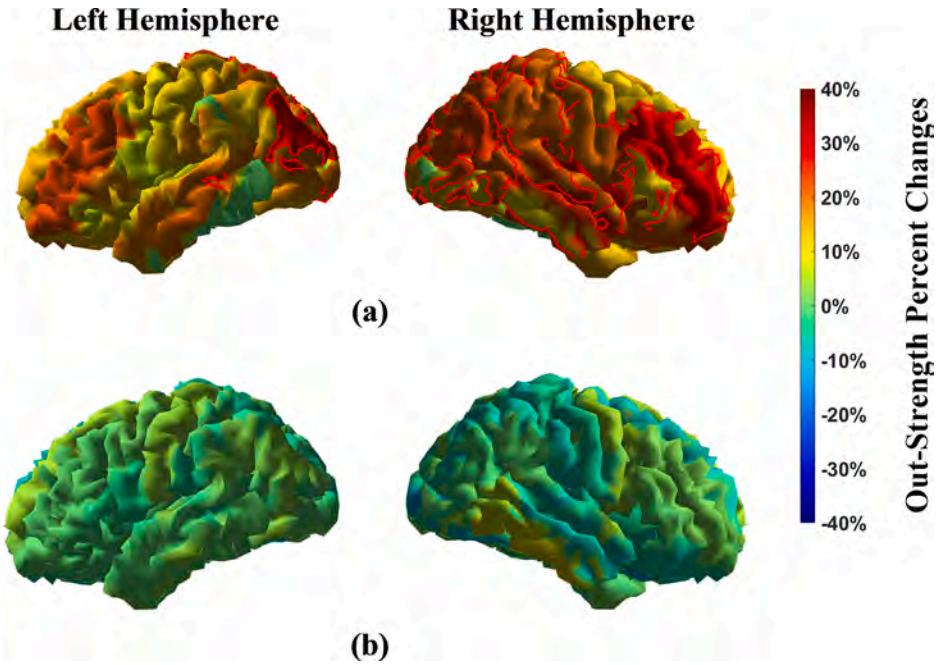

Fig. 5. Brain map of out-strength percentage change between anxious and non-anxious depressive groups for eyes-open condition (a) and eyes-closed condition (b). The regions showing significant differences are enclosed with red and blue contours ($p < 0.05$). (For interpretation of the references to colour in this figure legend, the reader is referred to the web version of this article.)

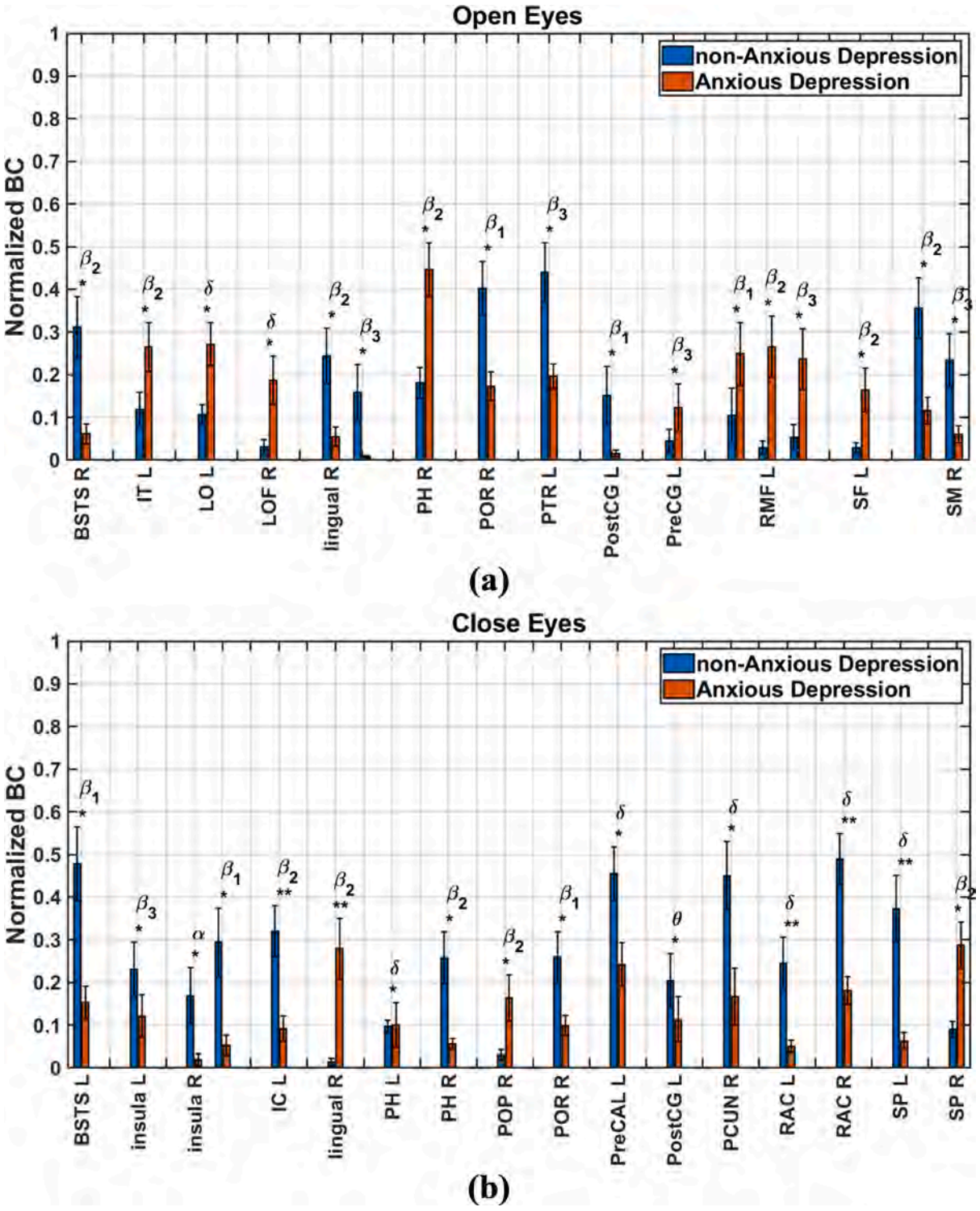

Fig. 6. Bar plot of selected BC features for eyes-open condition (a) and eyes-closed condition (b). Single asterisk denotes $p < 0.05$, and double asterisks denote $p < 0.01$. (BSTS: banks of superior temporal sulcus, IT: inferior temporal gyrus, LO: lateral occipital sulcus, LOF: lateral orbitofrontal cortex, PH: parahippocampal gyrus, POR: pars orbitalis, PTR: pars triangularis, PostCG: postcentral gyrus, RMF: rostral middle frontal gyrus, SF: superior frontal gyrus, SM: supramarginal gyrus, IC: isthmus cingulate gyrus, POP: pars opercularis, PreCAL: pericalcarine, PCUN: precuneus, RAC: rostral anterior cingulate cortex, SP: superior parietal).

the right middle temporal gyrus and right medial orbitofrontal cortex decreased significantly. Also, the spatial distribution of node centrality demonstrates nodes with significant lower BC in the medial and lateral parietal (precuneus, supramarginal, and isthmus cingulate gyri) and bilateral rostral anterior cingulate as well as higher BC in the left superior frontal gyrus and bilateral parahippocampal gyri (see Fig. 8(c)).

3.4. Classification results

The SVM was used to determine which graph theory feature is capable of discrimination between anxious and non-anxious depressive groups. To evaluate the performance of SVM applied on each input matrix, we compared the values of accuracy, F-score, and specificity in

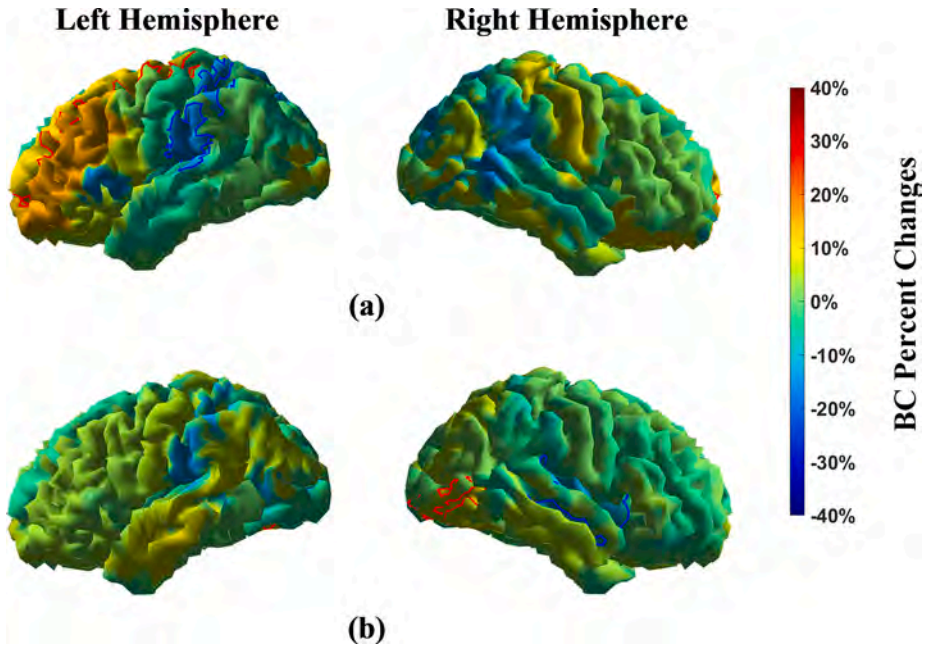

Fig. 7. Brain map of BC percentage change between anxious and non-anxious depressive groups for eyes-open condition (a) and eyes-closed condition (b). The regions showing significant differences are enclosed with red and blue contours ($p < 0.05$). (For interpretation of the references to colour in this figure legend, the reader is referred to the web version of this article.)

Table 2. Compared with in-strength and BC, the out-strength feature achieved higher accuracy, F-score, and specificity in both states while the highest results were obtained in the eyes-closed condition with 91.66% accuracy, 87.5% F-score, and 100% specificity. On the other hand, in-strength outperformed BC features in the eyes-open state but resulted in roughly similar performance with BC in the eyes-closed condition. In addition, according to Table 2, the features of strength and BC resulted in higher accuracy, F-score, and specificity in the eyes-closed state compared to the eyes-open state.

4. Discussion

In this study, we analyzed the connectivity strength and centrality of the directed network within 68 cortical regions in MDD patients with and without anxiety. The classification results showed that out-strength features performed better than in-strength and BC features in the separation of the depressive groups. We also investigated the effect of eyes open and closed conditions on resting-state EEG for discriminating anxious and non-anxious depressive patients. Compared with the classification results of the eyes-open state, we found that the SVM achieved a higher accuracy, F-score, and specificity in the eyes-closed state for all features, although more statistically different features were observed in the eyes-open condition for connectivity strength. These results proved that not only the information flow between cortical regions is changed in both directions, but also the brain network is altered in different resting states. As other studies claimed a similar interpretation including asymmetric information flow between the left and right hemispheres in MDD patients and altered resting-state EEG in eyes open and closed conditions for MDD patients [27,43].

The topographic maps demonstrate that the out-strength across a large proportion of the brain in the low-to-high frequency bands for the anxious depressive group is greater during the eyes-open recording. This implies that the increased outward information flow might reflect the presence of comorbid anxiety in MDD patients. On the other hand, the inward information flow to some certain ROIs including fronto-central regions (bilateral postcentral, left caudal middle frontal, and left pars triangularis gyri), and right precuneus increased substantially in low-to-high frequency bands for eyes-open anxious depressed individuals. This result is somewhat consistent with what other studies have achieved since they have reported that anxious depressed subjects have higher functional connectivity at the middle frontal gyrus and the precuneus [13,14]. Furthermore, we found that, during eyes-closed condition, the information flow of a few ROIs exhibited significant differences such as the left precentral gyrus where the in-strength reduced predominantly in the anxious depressive group, it is while a study suggested that the functional connectivity in such group increases at the right precentral gyrus [14].

Our statistical analysis also showed that the out-strength changes become stronger in the right hemisphere. The out-strength over almost half of the right frontal, right temporal, and right parieto-occipital lobes in the anxious depressive group increased significantly. Several studies have repeatedly reported abnormal changes in the right hemisphere for anxious depressed patients such as increased activation in the right frontal and right parieto-temporal regions [17–19,21]. In addition, apart from the studies that have taken into account both depression and anxiety, some studies have also confirmed that the dysfunction of the right hemisphere is associated with MDD patients in comparison to healthy controls [27,44].

Another important finding of this study indicates that the brain network disruption is mainly related to the beta bands (beta 1, beta 2, and beta 3) in which the cingulate cortex, posterior regions (right lingual gyrus, right precuneus, and bilateral pericalcarine), frontal regions (rostral middle frontal and left pars triangularis), the motor cortex (left paracentral, left precentral and bilateral postcentral gyri), temporal lobe and insula displayed significant difference. There is also some evidence of increased beta activity in the entire brain region for MDD patients with comorbid anxiety and high-beta power at the fronto-temporal for the non-anxious depressive group and the posterior cortices for the anxious depressive group [22,23,45]. It is further stated that the prominence of beta bands may lead to anxiety and stress, while its suppression may cause depression and poor cognition [46]. These findings indicate the role of the beta band to distinguish anxious or non-anxious depressions.

Based on the BC results, we observed multiple brain regions have been changed significantly. Some of these observations are consistent with the results of other studies. For example, a study found an increased

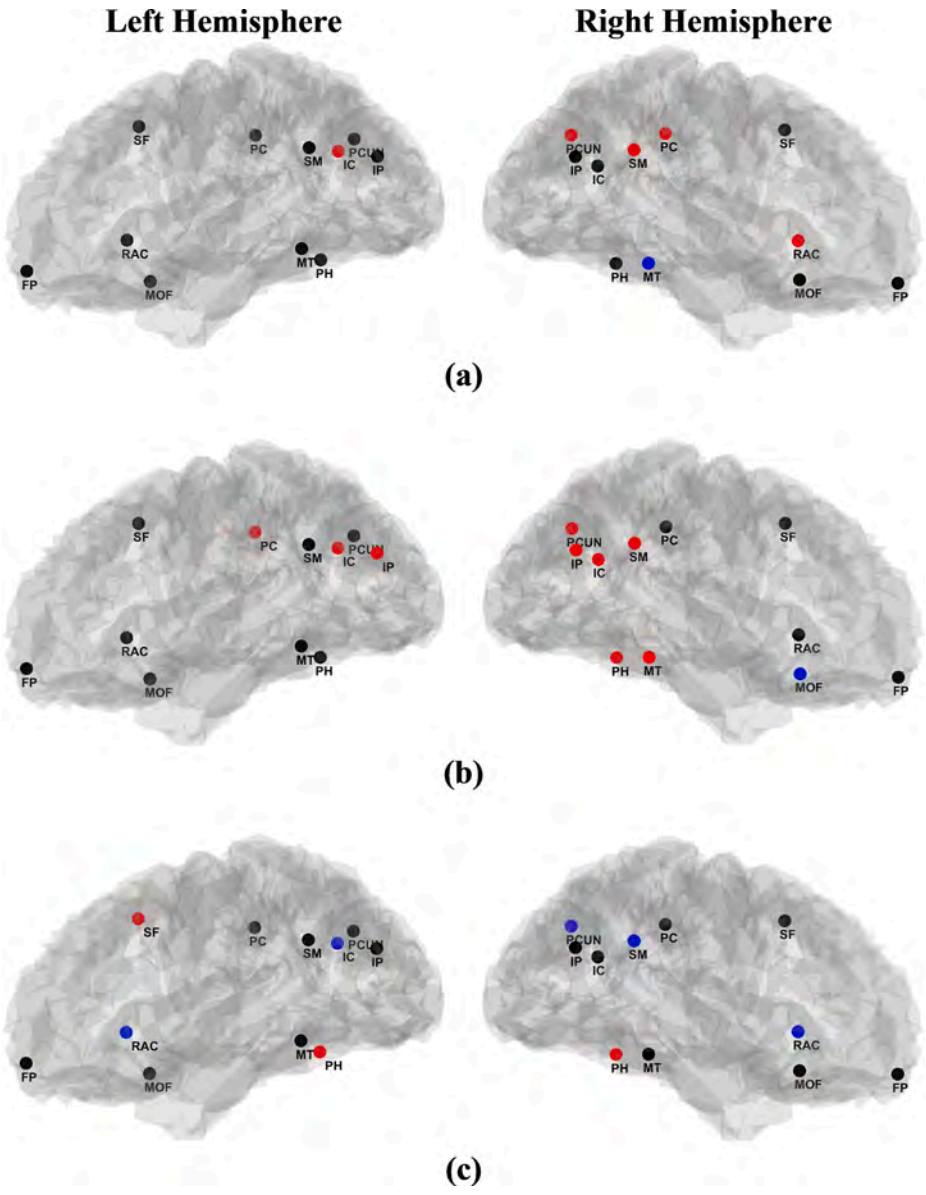

Fig. 8. Anatomical locations of regions indicating significant difference ($p < 0.05$) in in-strength (a), out-strength (b), and BC (c) within the default mode network (DMN). Red nodes: increased values of network metrics in the anxious depressive group. Blue nodes: decreased values of network metrics in the anxious depressive group. Black nodes: DMN nodes that did not change significantly. (For interpretation of the references to colour in this figure legend, the reader is referred to the web version of this article.)

Table 2
Classification results between anxious and non-anxious depressive groups for both conditions based on the selected in-strength, out-strength and BC features.

	Eyes Open Condition			Eyes Close Condition		
	Accuracy	F-score	Specificity	Accuracy	F-score	Specificity
in-Strength	66.66%	60%	66.66%	75%	66.66%	80%
out-Strength	79.16%	66.66%	93.33%	91.66%	87.5%	100%
BC	58.33%	54.54%	53.33%	75%	70%	73.33%

nodal centrality in the left postcentral and right supramarginal gyri for the non-anxious depressive group [47]. This study also suggested that the nodal centrality in the bilateral lingual gyrus decreased for MDD patients. According to our results, this finding was observed only in the right lingual gyrus during the eyes-closed state. Furthermore, our preliminary results revealed that the BC in the left superior frontal gyrus increased for the anxious depressive group but decreased in the bilateral insula. In subsequent research work, abnormal neural activities in the bilateral superior frontal gyrus and insula for anxious depression patients have also been reported [10]. The present study also claims that the BC in the left lateral occipital cortex increases for the anxious depressive group. Further support for this finding can be found in another fMRI study. In particular, a cortical thinning in the left lateral occipital cortex for the anxious depressive group was reported [11].

In addition to graph analysis (i.e., connectivity strength and betweenness centrality), we identified the overlapped contrast regions with the regions of the default mode network to assess the differences in brain activity between anxious and non-anxious depressive patients. Our prominent result indicated that only the supramarginal and isthmus cingulate gyri, as two main components in the posterior area of DMN, showed a significant difference in terms of inward and outward connectivity strength, and betweenness centrality. However, most nodes in

the posterior of DMN showed increased connectivity strength in both directions for anxious depressive patients but decreased node centrality. Similarly, a study observed increased functional connectivity in the posterior of DMN in anxious depressive elderly patients [13].

All in all, various brain regions in different frequency bands showed significant differences in the two groups of depression. Some brain regions exhibited constant significant differences in all network features of strength and BC. As evident in the results, the network features in the left postcentral gyrus were changed significantly in open eyes recording. This region as a part of the somatosensory cortex plays a key role in emotional processing and is associated with anxiety disorder [48]. The right supramarginal gyrus is another crucial region that also differed in open-eye condition. It is reported that disrupting neural networks in the right supramarginal gyrus has a detrimental influence on the sense of empathy and makes people more egocentric [49]. Moreover, several significant differences in features of the network were observed in the right insula and pars orbitalis, which both involve semantic and emotional processing, and thereby impairment in such regions brings about anxiety and depression [50–53].

Our study is not devoid of limitations. First, we did not include the healthy control group in our experiment since we only attempted to provide a picture of different brain networks between anxious and non-anxious depressive groups. Second, the patient population size in each group was small. Therefore, a large number of patients are required to verify the robustness of the results. Third, the quality of source estimation could be significantly improved if we utilized a high number of EEG channels such as a recording system with dense electrode arrays (i.e. 64–256 electrodes). Finally, we considered two of the most common graph metrics including connectivity strength and betweenness centrality for the assessment of brain network function and hub nodes (highly connected brain areas). It is suggested in future research to consider other features of the graph network such as the clustering coefficient, which may offer other aspects of brain networks in MDD patients with and without comorbid anxiety.

5. Conclusion

To the best of our knowledge, this is the first study that has investigated differences in the directed brain network in anxious and non-anxious depressed patients using an effective connectivity measure and the EEG source connectivity method. Network metrics comprising directed node strength and BC were analyzed by a statistical test and the machine learning approach. Classification results demonstrate outward connectivity strength had the highest performance in separating the two groups of patients, while all features performed better in the eyes-closed state than in the eyes-open state. Our main findings related to the strength of connectivity consist of increased node strength during the eyes-open condition, especially a higher out-strength in the right hemisphere for the anxious depressive group. In addition, we found that beta oscillations reflect the most altered brain network in terms of node strength and BC. Further analysis revealed that connectivity and centrality in most regions of posterior DMN were changed significantly. To conclude, the obtained results could potentially lead to the understanding of the underlying brain network of patients with comorbid depression-anxiety disorder, however, more research still is needed regarding the anxious depressive disorder.

CRediT authorship contribution statement

Hesam Shokouh Alaei: Conceptualization, Methodology, Software, Validation, Formal analysis, Data curation, Writing – original draft, Visualization. **Majid Ghoshuni:** Conceptualization, Methodology, Validation, Investigation, Writing – review & editing, Supervision, Project administration. **Iraj Vosough:** Investigation, Resources.

Declaration of Competing Interest

The authors declare that they have no known competing financial interests or personal relationships that could have appeared to influence the work reported in this paper.

Data availability

Data will be made available on request.

Acknowledgement

This research did not receive any specific grant from funding agencies in the public, commercial, or not-for-profit sectors.

References

[1] E. Bromet, L.H. Andrade, I. Hwang, N.A. Sampson, J. Alonso, G. de Girolamo, R. de Graaf, K. Demyttenaere, C. Hu, N. Iwata, A.N. Karam, J. Kaur, S. Kostyuchenko, J.-P. Lépine, D. Levinson, H. Matschinger, M.E.M. Mora, M.O. Browne, J. Posada-Villa, M.C. Viana, D.R. Williams, R.C. Kessler, Cross-national epidemiology of DSM-IV major depressive episode, BMC Med. 9 (2011) 90, https://doi.org/10.1186/1741-7015-9-90.

[2] R.C. Kessler, C.B. Nelson, K.A. McGonagle, J. Liu, M. Swartz, D.G. Blazer, Comorbidity of DSM-III-R major depressive disorder in the general population: results from the US National Comorbidity Survey, Br. J. Psychiatry. Suppl (1996) 17–30.

[3] S. Mineka, D. Watson, L.A. Clark, Comorbidity of anxiety and unipolar mood disorders, Annu. Rev. Psychol. 49 (1998) 377–412, https://doi.org/10.1146/annurev.psych.49.1.377.

[4] R.M.A. Hirschfeld, The comorbidity of major depression and anxiety disorders: recognition and management in primary care, Prim. Care Companion J. Clin. Psychiatry. 3 (2001) 244–254, https://doi.org/10.4088/pcc.v03n0609.

[5] J.M. Gorman, Comorbid depression and anxiety spectrum disorders, Depress Anxiety. 4 (1996) 160–168, https://doi.org/10.1002/(SICI)1520-6394(1996)4:4<160::AID-DA2>3.0.CO;2-J.

[6] M.-J. van Tol, L.R. Demenescu, N.J.A. van der Wee, R. Kortekaas, N. Marjan M.A., J.A. Den Boer, R.J. Renken, M.A. van Buchem, F.G. Zitman, A. Aleman, D.J. Veltman, Functional magnetic resonance imaging correlates of emotional word encoding and recognition in depression and anxiety disorders, Biol. Psychiatry. 71 (2012) 593–602. <https://doi.org/10.1016/j.biopsych.2011.11.016>.

[7] M.-J. van Tol, N.J.A. van der Wee, O.A. van den Heuvel, M.M.A. Nielen, L. R. Demenescu, A. Aleman, R. Renken, M.A. van Buchem, F.G. Zitman, D. J. Veltman, Regional brain volume in depression and anxiety disorders, Arch. Gen. Psychiatry. 67 (2010) 1002–1011, https://doi.org/10.1001/archgenpsychiatry.2010.121.

[8] M.J. van Tol, N.J.A. van der Wee, L.R. Demenescu, M.M.A. Nielen, A. Aleman, R. Renken, M.A. van Buchem, F.G. Zitman, D.J. Veltman, Functional MRI correlates of visuospatial planning in out-patient depression and anxiety, Acta Psychiatr. Scand. 124 (2011) 273–284, https://doi.org/10.1111/j.1600-0447.2011.01702.x.

[9] J.L. Stewart, E.J. White, R. Kuplicki, E. Akeman, J. Bodurka, Y.-H. Cha, J. S. Feinstein, S.S. Khalsa, J.B. Savitz, T.A. Victor, M.P. Paulus, R.L. Aupperle, Women with major depressive disorder, irrespective of comorbid anxiety disorders, show blunted bilateral frontal responses during win and loss anticipation, J. Affect. Disord. 273 (2020) 157–166, https://doi.org/10.1016/j.jad.2020.04.064.

[10] U. Lueken, B. Straube, Y. Yang, T. Hahn, K. Beesdo-Baum, H.-U. Wittchen, C. Konrad, A. Ströhle, A. Wittmann, A.L. Gerlach, B. Pfleiderer, V. Arolt, T. Kircher, Separating depressive comorbidity from panic disorder: a combined functional magnetic resonance imaging and machine learning approach, J. Affect. Disord. 184 (2015) 182–192, https://doi.org/10.1016/j.jad.2015.05.052.

[11] E. Canu, M. Kostić, F. Agosta, A. Munjiza, P.M. Ferraro, D. Pesic, M. Copetti, A. Peljto, D.L. Tosevski, M. Filippi, Brain structural abnormalities in patients with major depression with or without generalized anxiety disorder comorbidity, J. Neurol. 262 (2015) 1255–1265, https://doi.org/10.1007/s00415-015-7701-z.

[12] B. Kim, M.-K. Kim, E. Yoo, J.-Y. Lee, A.Y. Choe, K.-H. Yook, K.S. Lee, T.K. Choi, S.-H. Lee, Comparison of panic disorder with and without comorbid major depression by using brain structural magnetic resonance imaging, Prog. Neuro-Psychopharmacol. Biol. Psychiatry. 43 (2013) 188–196, https://doi.org/10.1016/j.pnpbp.2012.12.022.

[13] C. Andreescu, M. Wu, M.A. Butters, J. Figurski, C.F. Reynolds, H.J. Aizenstein, The default mode network in late-life anxious depression, Am. J. Geriatr. Psychiatry. 19 (2011) 980–983, https://doi.org/10.1097/JGP.0b013e318227f4f9.

[14] J.N. Pannekoek, S.J.A. van der Werff, M.J. van Tol, D.J. Veltman, A. Aleman, F. G. Zitman, S.A.R.B. Rombouts, N.J.A. van der Wee, Investigating distinct and common abnormalities of resting-state functional connectivity in depression, anxiety, and their comorbid states, Eur. Neuropsychopharmacol. 25 (2015) 1933–1942, https://doi.org/10.1016/j.euroneuro.2015.08.002.

[15] C. He, L. Gong, Y. Yin, Y. Yuan, H. Zhang, L. Lv, X. Zhang, J.C. Soares, H. Zhang, C. Xie, Z. Zhang, Amygdala connectivity mediates the association between anxiety and depression in patients with major depressive disorder, Brain Imag. Behav. 13 (2019) 1146–1159, https://doi.org/10.1007/s11682-018-9923-z.

[16] L. Delaparte, F.-C. Yeh, P. Adams, A. Malchow, M.H. Trivedi, M.A. Oquendo, T. Deckersbach, T. Ogden, D.A. Pizzagalli, M. Fava, C. Cooper, M. McInnis, B. T. Kurian, M.M. Weissman, P.J. McGrath, D.N. Klein, R.V. Parsey, C. DeLorenzo, A comparison of structural connectivity in anxious depression versus non-anxious depression, J. Psychiatr. Res. 89 (2017) 38–47, https://doi.org/10.1016/j.jpsychires.2017.01.012.

[17] G.E. Bruder, R. Fong, C.E. Tenke, P. Leite, J.P. Towey, J.E. Stewart, P.J. McGrath, F.M. Quitkin, Regional brain asymmetries in major depression with or without an anxiety disorder: a quantitative electroencephalographic study, Biol. Psychiatry. 41 (1997) 939–948, https://doi.org/10.1016/S0006-3223(96)00260-0.

[18] D.A. Pizzagalli, J.B. Nitschke, T.R. Oakes, A.M. Hendrick, K.A. Horras, C.L. Larson, H.C. Abercrombie, S.M. Schaefer, J.V. Koger, R.M. Benca, R.D. Pascual-Marqui, R. J. Davidson, Brain electrical tomography in depression: the importance of symptom severity, anxiety, and melancholic features, Biol. Psychiatry. 52 (2002) 73–85, https://doi.org/10.1016/s0006-3223(02)01313-6.

[19] L. Feldmann, C.E. Piechaczek, B.D. Grünewald, V. Pehl, J. Bartling, M. Frey, G. Schulte-Körne, E. Greimel, Resting frontal EEG asymmetry in adolescents with major depression: impact of disease state and comorbid anxiety disorder, Clin. Neurophysiol. 129 (2018) 2577–2585, https://doi.org/10.1016/j.clinph.2018.09.028.

[20] L.M. Kentgen, C.E. Tenke, D.S. Pine, R. Fong, R.G. Klein, G.E. Bruder, Electroencephalographic asymmetries in adolescents with major depression: influence of comorbidity with anxiety disorders, J. Abnorm. Psychol. 109 (2000) 797–802, https://doi.org/10.1037//0021-843x.109.4.797.

[21] D. Mathersul, L.M. Williams, P.J. Hopkinson, A.H. Kemp, Investigating models of affect: relationships among EEG alpha asymmetry, depression, and anxiety, Emotion. 8 (2008) 560–572, https://doi.org/10.1037/a0012811.

[22] S.-Y. Wang, I.-M. Lin, S.-Y. Fan, Y.-C. Tsai, C.-F. Yen, Y.-C. Yeh, M.-F. Huang, Y. Lee, N.-M. Chiu, C.-F. Hung, P.-W. Wang, T.-L. Liu, H.-C. Lin, The effects of alpha asymmetry and high-beta down-training neurofeedback for patients with the major depressive disorder and anxiety symptoms, J. Affect. Disord. 257 (2019) 287–296, https://doi.org/10.1016/j.jad.2019.07.026.

[23] V. Paquette, M. Beauregard, D. Beaulieu-Prévost, Effect of a psychoneurotherapy on brain electromagnetic tomography in individuals with major depressive disorder, Psychiat. Res. Neuroimag. 174 (2009) 231–239, https://doi.org/10.1016/j.pscychresns.2009.06.002.

[24] R. Nusslock, A.J. Shackman, B.W. McMenamin, L.L. Greischar, R.J. Davidson, M. Kovacs, Comorbid anxiety moderates the relationship between depression history and prefrontal EEG asymmetry, Psychophysiology. 55 (2018) e12953.

[25] J.L. Koberda, Chapter 5 – Z-score LORETA neurofeedback as a potential therapy in depression/anxiety and cognitive Dysfunction1www.TallahasseeNeuroBalanceCenter.com, in: R.W. Thatcher, J.F.B.T.-Z.S.N. Lubar (Eds.), Academic Press, San Diego, 2015: pp. 93–113. <https://doi.org/10.1016/B978-0-12-801291-8.00005-4>.

[26] S. Liu, S. Chen, Z. Huang, X. Liu, M. Li, F. Su, X. Hao, D. Ming, Hypofunction of directed brain network within alpha frequency band in depressive patients: a graph-theoretic analysis, Cogn. Neurodyn. 16 (2022) 1059–1071, https://doi.org/10.1007/s11571-022-09782-6.

[27] F. Hasanzadeh, M. Mohebbi, R. Rostami, Graph theory analysis of directed functional brain networks in major depressive disorder based on EEG signal, J. Neural Eng. 17 (2020) 26010, https://doi.org/10.1088/1741-2552/ab7613.

[28] D.A. Chandler, A. Roach, A. Ellison, E. Husid Burton, L. Jelsone-Swain, Symptoms of depression together with trait anxiety increase the ability to predict alpha power change between attention and resting states, Int. J. Psychophysiol. 182 (2022) 57–69, https://doi.org/10.1016/j.ijpsycho.2022.09.010.

[29] Y. Zhang, L. Lei, Z. Liu, M. Gao, Z. Liu, N. Sun, C. Yang, A. Zhang, Y. Wang, K. Zhang, Theta oscillations: a rhythm difference comparison between major depressive disorder and anxiety disorder, Front. Psychiatry. 13 (2022). https://www.frontiersin.org/articles/10.3389/fpsyt.2022.827536.

[30] M. Hassan, F. Wendling, Electroencephalography source connectivity: aiming for high resolution of brain networks in time and space, IEEE Signal Process. Mag. 35 (2018) 81–96, https://doi.org/10.1109/MSP.2017.2777518.

[31] R. Pascual-Marqui, Discrete, 3D distributed, linear imaging methods of electric neuronal activity. Part 1: Exact, zero error localization, Math. Phys. Biol. Phys. Neurons Cogn. 0710 (2007).

[32] L.R. Derogatis, R.S. Lipman, L. Covi, SCL-90: an outpatient psychiatric rating scale–preliminary report, Psychopharmacol. Bull. 9 (1973) 13–28.

[33] S. Baillet, J.C. Mosher, R.M. Leahy, Electromagnetic brain mapping, IEEE Signal Process. Mag. 18 (2001) 14–30, https://doi.org/10.1109/79.962275.

[34] T.F. Oostendorp, A. van Oosterom, Source parameter estimation in inhomogeneous volume conductors of arbitrary shape, IEEE Trans. Biomed. Eng. 36 (1989) 382–391, https://doi.org/10.1109/10.19859.

[35] R. Oostenveld, P. Fries, E. Maris, J.-M. Schoffelen, FieldTrip: Open source software for advanced analysis of MEG, EEG, and invasive electrophysiological data, Comput. Intell. Neurosci. 2011 (2011), 156869, https://doi.org/10.1155/2011/156869.

[36] B. Fischl, FreeSurfer, Neuroimage. 62 (2012) 774–781, https://doi.org/10.1016/j.neuroimage.2012.01.021.

[37] R.S. Desikan, F. Ségonne, B. Fischl, B.T. Quinn, B.C. Dickerson, D. Blacker, R. L. Buckner, A.M. Dale, R.P. Maguire, B.T. Hyman, M.S. Albert, R.J. Killiany, An automated labeling system for subdividing the human cerebral cortex on MRI scans into gyral based regions of interest, Neuroimage. 31 (2006) 968–980, https://doi.org/10.1016/j.neuroimage.2006.01.021.

[38] M. Rubinov, O. Sporns, Complex network measures of brain connectivity: uses and interpretations, Neuroimage. 52 (2010) 1059–1069, https://doi.org/10.1016/j.neuroimage.2009.10.003.

[39] A. Fornito, A. Zalesky, E.T.B.T.-F. of B.N.A. Bullmore, eds., Chapter 3 – Connectivity Matrices and Brain Graphs, in: Academic Press, San Diego, 2016, pp. 89–113. <https://doi.org/10.1016/B978-0-12-407908-3.00003-0>.

[40] M.J. Kaminski, K.J. Blinowska, A new method of the description of the information flow in the brain structures, Biol. Cybern. 65 (1991) 203–210, https://doi.org/10.1007/BF00198091.

[41] T. Schneider, A. Neumaier, Algorithm 808: ARfit - a MATLAB package for the estimation of parameters and eigenmodes of multivariate autoregressive models, ACM Trans. Math. Softw. (2000), https://doi.org/10.1145/382043.382316.

[42] A. Perinelli, D. Tabarelli, C. Miniussi, L. Ricci, Dependence of connectivity on geometric distance in brain networks, Sci. Rep. 9 (2019) 13412, https://doi.org/10.1038/s41598-019-50106-2.

[43] S. Liu, X. Liu, D. Yan, S. Chen, Y. Liu, X. Hao, W. Ou, Z. Huang, F. Su, F. He, D. Ming, Alterations in patients with first-episode depression in the eyes-open and eyes-closed conditions: a resting-state EEG study, IEEE Trans. Neural Syst. Rehabil. Eng. 30 (2022) 1019–1029, https://doi.org/10.1109/TNSRE.2022.3166824.

[44] P. Flor-Henry, Lateralized temporal-limbic dysfunction and psychopathology*, Ann. N. Y. Acad. Sci. 280 (1976) 777–795, https://doi.org/10.1111/j.1749-6632.1976.tb25541.x.

[45] I.-M. Lin, T.-C. Chen, H.-Y. Lin, S.-Y. Wang, J.-L. Sung, C.-W. Yen, Electroencephalogram patterns in patients comorbid with major depressive disorder and anxiety symptoms: Proposing a hypothesis based on hypercortical arousal and not frontal or parietal alpha asymmetry, J. Affect. Disord. 282 (2021) 945–952, https://doi.org/10.1016/j.jad.2021.01.001.

[46] P.A. Abhang, B.W. Gawali, S.C. Mehrotra, Chapter 3 – technical aspects of brain rhythms and speech parameters, in: P.A. Abhang, B.W. Gawali, S.C.B.T.-I. to E.S.-B. E.R. Mehrotra (Eds.), Academic Press, 2016, pp. 51–79. <https://doi.org/10.1016/B978-0-12-804490-2.00003-8>.

[47] J. Zhang, J. Wang, Q. Wu, W. Kuang, X. Huang, Y. He, Q. Gong, Disrupted brain connectivity networks in drug-naive, first-episode major depressive disorder, Biol. Psychiatry. 70 (2011) 334–342, https://doi.org/10.1016/j.biopsych.2011.05.018.

[48] X. Li, M. Zhang, K. Li, F. Zou, Y. Wang, X. Wu, H. Zhang, The altered somatic brain network in state anxiety, Front. Psychiatry. 10 (2019). https://www.frontiersin.org/articles/10.3389/fpsyt.2019.00465.

[49] G. Silani, C. Lamm, C.C. Ruff, T. Singer, Right supramarginal gyrus is crucial to overcome emotional egocentricity bias in social judgments, J. Neurosci. 33 (2013), https://doi.org/10.1523/JNEUROSCI.1488-13.2013.

[50] M.B. Stein, A.N. Simmons, J.S. Feinstein, M.P. Paulus, Increased amygdala and insula activation during emotion processing in anxiety-prone subjects, Am. J. Psychiatry. 164 (2007) 318–327, https://doi.org/10.1176/ajp.2007.164.2.318.

[51] D. Sliz, S. Hayley, Major depressive disorder and alterations in insular cortical activity: a review of current functional magnetic imaging research, Front. Hum. Neurosci. 6 (2012). https://www.frontiersin.org/articles/10.3389/fnhum.2012.00323.

[52] M. Belyk, S. Brown, J. Lim, S.A. Kotz, Convergence of semantics and emotional expression within the IFG pars orbitalis, Neuroimage. 156 (2017) 240–248, https://doi.org/10.1016/j.neuroimage.2017.04.020.

[53] K. Zhao, H. Liu, R. Yan, L. Hua, Y. Chen, J. Shi, Q. Lu, Z. Yao, Cortical thickness and subcortical structure volume abnormalities in patients with major depression with and without anxious symptoms, Brain Behav. 7 (2017) e00754.